Bioelectromagnetics 22:487–493 (2001)

Frequency Response of Alternating Currents through the *Staphylococcus aureus* α-hemolysin Ion Channel

M. Misakian,[1]* J.J. Kasianowicz,[2] B. Robertson,[1] and O. Petersons[1]

[1]*NIST, Electricity Division, Gaithersburg, Maryland*

[2]*NIST, Biotechnology Division, Gaithersburg, Maryland*

Alternating currents were measured through transmembrane ion channels formed by *Staphylococcus aureus* α-hemolysin proteins in planar bilayer membranes as part of an investigation to determine the channel's frequency response and the appropriateness of an equivalent circuit commonly used to model electrical interactions at the surface of cells. The experimental approach includes a novel method for separating the alternating current through one or more channels, which is conductive in nature, from the capacitively coupled current through the membrane. Separation of the conductive and capacitive alternating currents made it possible to measure the frequency response of the α-hemolysin channels. The results of the study are consistent with an equivalent circuit of a membrane capacitor in parallel with one or more channel resistors over the frequency range 30–120 Hz. The possible usefulness of frequency response data for ion channels in cell membranes during investigations of biological effects of time-varying magnetic fields is briefly discussed. Bioelectromagnetics 22:487–493, 2001. Published 2001 Wiley-Liss, Inc.†

Key words: electrical properties; membrane; ion transport; planar membranes; equivalent circuit

INTRODUCTION

An electrically equivalent circuit model that has been commonly used to describe biological membranes with ion channels is that of a capacitor, representing the membrane, in parallel with one or more resistors, representing the channel(s) [Hille, 1991]. This paper considers the appropriateness of the above model for a planar bilayer lipid membrane with transmembrane protein channels formed by *Staphylococcus aureus* α-hemolysin (αHL) proteins [Menestrina, 1986; Bezrukov and Kasianowicz, 1993; Kasianowicz and Bezrukov, 1995; Bezrukov et al., 1996; Song et al., 1996; Bezrukov and Kasianowicz, 1997; Kasianowicz et al., 1999; Henrickson et al., 2000] when DC and combined DC and AC potentials are applied across the membrane. In particular, the resistive character of the channel is examined by measuring the frequency response of alternating current through one or more channels.

This paper presents measurements that separate the steady state alternating ion current through the αHL channels from the capacitively coupled alternating current through the bilayer membrane. The ability to distinguish between the two kinds of alternating currents may be important in bioeffects research because currents through channels represent transport of ions through the membrane, while capacitively coupled currents do not. Measurement of the conductive AC current solely through the channel during the present investigation made it possible to determine the frequency response of the channel, a primary objective of the paper. As will be discussed later, frequency response data for ion channels may be important during investigations of biological effects of cells exposed to time-varying magnetic fields.

The experimental approach used in the present study differs from impedance spectroscopy [Macdonald, 1987; Covington and Zhou, 1992; Deslouis et al., 1994; Benavente et al., 1998], which lead to plots of the real and imaginary equivalent circuit impedances in the complex plane as a function of frequency (Nyquist plots). In the present context, the "real impedance" would correspond to channel

Contract grant sponsors: Office of the Utility Technologies, U.S. Department of Energy.

*Correspondence to: Dr. Martin Misakian, NIST, 100 Bureau Drive, MS 8113, Gaithersburg, Maryland 20899-8113.
E-mail: martin.misakian@nist.gov

Received for review 29 July, 2000; Final revision received 20 January 2001

resistance. We note that two earlier studies reported in Bioelectromagnetics of ion transport through ion channels [Galt et al., 1993] and membranes [Durney et al., 1993] during simultaneous application of AC and DC magnetic fields involved measurements of only DC ion currents. The focus of these earlier studies was related to examining the validity of certain resonance models for biological effects.

In the present study, we chose the αHL channel, in part, because unlike many voltage-gated channels, the αHL channel can remain open for extended periods [Kasianowicz and Bezrukov, 1995; Kasianowicz et al., 1996] expediting the acquisition of data and demonstrating the current-separation technique described below.

APPARATUS AND MATERIALS

A schematic view of the chamber and a portion of the measurement circuitry is shown in Figure 1. The experimental chamber is a close copy of one used by Bezrukov and Kasianowicz [1993] and is fabricated from polytetrafluoroethylene (PTFE). Partitions made of PTFE, 0.025 mm thick with hole diameters that varied from about 60 to 100 μm, were used to divide the chamber in two halves. Bilayer lipid membranes are formed across the hole in a manner described below. During the measurements, each half of the chamber was filled with a 1 M KCl (1 mol/L)[1] bath (5 mM HEPES buffer, pH 7.5) to a level just above the hole in the partition. An operational amplifier (OP77) sums the AC and DC voltages that are applied across the PTFE partition and membrane with Ag/AgCl electrodes (In Vivo Metrics, Healdsburg, CA)[2] surrounded by 3 M KCl agar barriers. During some measurements, one or both electrodes were in direct contact with the KCl bath, but the absence of the agar barrier did not significantly influence the results.

The current through the membrane and ion channels is determined using the current-to-voltage converter shown in Figure 1 (Burr-Brown OPA128). The relationship between the direct current through one or more channels arriving at the input of OPA128, I_{dc}, and the output voltage, V_{dco}, is given by the expression [Peyton and Walsh, 1993]

$$I_{dc} = -\frac{V_{dco}}{R_f}, \tag{1}$$

[1]The SI unit of solute concentration is mol/L.

[2]The identification of commercial materials and their sources in this paper is made to adequately describe the experimental results. In no case does this identification imply recommendation by the National Institute of Standards and Technology, nor does it imply that the material is the best available.

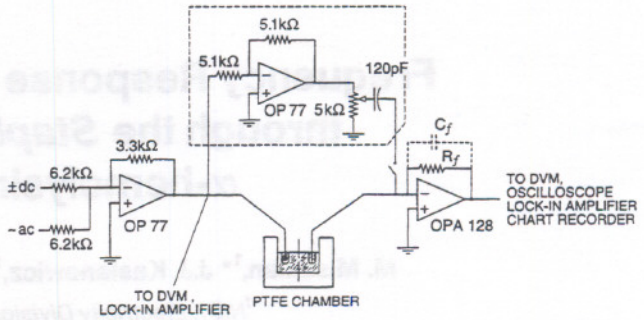

Fig. 1. Schematic drawing of the experimental chamber and a portion of the measurement circuit. The circuit for canceling the capacitively coupled current (in dashed box) could be disabled with the switch.

where R_f is the feedback resistance and the minus sign is due to the phase inversion introduced by the operational amplifier. The corresponding relation between the alternating current, I_{ac}, and the alternating output voltage, V_{aco}, is similar but with the feedback impedance $R_f/[1 + (\omega R_f C_f)^2]^{1/2}$ taking the place of R_f, i.e.,

$$I_{ac} = \frac{V_{aco}}{R_f}\sqrt{1 + (\omega R_f C_f)^2}, \tag{2}$$

where the current and voltage are root mean square (rms) values, ω is equal to $2\pi f$, f is the frequency, and C_f is the stray capacitance in the feedback circuit of OPA128. The values of R_f and C_f are approximately 1.04 GΩ and 0.19 pF, respectively. The value of stray capacitance was determined by examining phase shifts of signals through OPA128 using a lock-in amplifier.

In order to measure the alternating current only through the channel, the portion of the circuit in the dashed box (Fig. 1), when enabled with the switch, is used to produce a second alternating current equal in magnitude but opposite in phase to cancel the capacitively coupled current from the membrane and partition. In this regard, we note that the capacitively coupled current from the membrane and partition has a phase shift of +90° with respect to the applied voltage while the alternating current through the channel is in phase with the voltage. Thus, to produce an alternating current opposite in phase to the membrane and partition current, the alternating current routed through the circuit in the dashed box must undergo a total phase shift of 270°. This shift is accomplished in two steps. First the inverting amplifier (OP77 with unity gain) introduces a phase shift of 180°. After the current passes the 120 pF capacitor, an additional 90° phase shift occurs. Consequently, when the "membrane/partition" and "OP77/120 pF" currents meet at the

input of OPA128, they differ in phase by 180°. Cancellation takes place by matching the magnitude of the two currents, which is done by varying the resistance of the 5 kΩ potentiometer until a minimum is observed in the AC signal from OPA128. This minimum signal, which represents the alternating current through the channel, is conveniently determined by minimizing the peak-to-peak amplitude of V_{aco} using an oscilloscope. Detecting the current through the channel using the above approach was necessary because the capacitively coupled current (tens of megohms impedance) was much greater than the current through a single channel ($\sim 10^9$ Ω resistance for our conditions), making the use of, for example, phase sensitive detection very difficult.

With the exception of the 5 kΩ potentiometer, the circuitry and PTFE chamber shown in Figure 1 were in a mu-metal box, and the box was located on a commercially available vibration isolation table to minimize electrical noise due to microphonics. The 5 kΩ potentiometer was external to the mu-metal box, electrically shielded, and connected to the rest of the circuit via a shielded cable.

MEMBRANE AND CHANNEL FORMATION

The lipid molecules for forming the membrane, 1,2-diphytanoyl-sn-Glycero-3-phosphocholine (Avanti Polar Lipids, Alabaster, AL) arrive at NIST in powder form and are stored at −80°C. When used for experiments, the powder (20 mg) is mixed with pentane (2 ml). The lipid bilayer is formed across the hole using a variation of a technique employed by Montal and Mueller [1972]. Initially, 1 M KCl solution partially fills each half of the chamber (volume: ~2.5 ml, surface area: ~0.97 cm^2). About 25 µl of lipid is applied to the KCl surfaces when the levels are just below the hole in the partition. The KCl levels are slowly raised in sequence to a point just above the hole to form the lipid bilayer. The additional KCl is introduced into the chamber via PTFE tubes connected between the chamber and syringes filled with KCl, and the process is monitored visually by observing the KCl levels through a microscope (not shown). During the raising of the KCl levels, an AC voltage is applied across the partition and the creation of the membrane is signaled by a sudden step-increase in the capacitively coupled current, I_{aco} (the current cancellation circuit is disabled during formation of the membrane). Prior to raising the KCl levels, the rim of the hole is coated with hexadecane using a solution of hexadecane in pentane (1:10 volume ratio). The pentane acts as a carrier for the hexadecane and evaporates within minutes, leaving a coating of hexadecane along the rim of the hole. The agar barrier for the Ag/AgCl electrodes and KCl solutions were prepared using deionized water.

Details of the experimental method for reconstituting the αHL ionic channel into the bilayer membrane are described elsewhere [Kasianowicz and Bezrukov, 1995; Kasianowicz et al., 1999]. Briefly, following formation of the membrane, 0.4–0.5 µl of αHL is added to the left half (*cis*) of the chamber (Fig. 1), while stirring, with an applied membrane potential of about plus or minus 60 mV. Creation of one or more ion channels is indicated when DC signals from OPA128 are observed using a chart recorder. The time between introduction of the αHL proteins and the creation of one or more channels varied from a few minutes to more than 30 min. The longer times typically occurred when smaller holes were used in the partition. All experiments were performed at room temperature, i.e., 22.5 ± 1°C. Introduction of the αHL was often delayed until drifts in the membrane capacitance became small.

EXPERIMENTAL APPROACH

In contrast to actual resistors, current–DC voltage characteristic curves for αHL channels can be nonlinear and partially rectifying [Krasilnikov, et al., 1988; Cescatti, et al., 1991]. Therefore, after the channel(s) formed, we first applied dc membrane potentials and measured the current–voltage curves of single and multiple channels for our conditions, because of their possible influence on the alternating current when combined AC and DC voltages are applied. If the channels behave similarly to resistors under alternating voltage conditions, one can expect the peak-to-peak values of the current to be influenced by the nonlinearity, as discussed in the next section.

Next, to determine the frequency response of the αHL channels, the capacitively coupled current was first canceled, and the current through one or more channels was measured as the frequency of the alternating current was varied. The frequency response was recorded for both positive and negative DC voltages. Because the rms value of alternating currents through an ideal resistor should be independent of frequency, the rms value of currents through one and multiple channels was examined for its constancy as the frequency was varied between 30 and 120 Hz.

During acquisition of data, no effort was made to control the number of channels that were formed following the formation of the first channel, e.g., by simultaneously purging the KCl with the αHL and adding fresh KCl to the chamber. Rather, when a certain number of channels were formed (one or more)

and when there was sufficient time before additional channels were created, the current–DC voltage characteristic curves were measured and frequency response measurements associated with a fixed number of channels were performed. Long lived single channels were more likely to occur when small diameter holes were used in the partition.

During the measurements of alternating currents through the channel(s), cancellation of the capacitively coupled current was frequently checked. However, drifts in the membrane capacitance likely went undetected at times, leading to greater leakage currents and consequently greater uncertainty in the value of the current through the channel(s). Uncertainties in the measurement of the AC and DC voltages were less than 1%.

RESULTS AND DISCUSSION

Prior to performing measurements with membranes and ion channels, simulation type measurements were made with resistors and capacitors in parallel to determine the effectiveness of the circuit for canceling the capacitively coupled current. For example, the capacitance corresponding to the membrane (and partition) and the resistance of a single channel in our system are roughly 55 pF and 1 GΩ, respectively. At frequencies of 120 and 30 Hz, the "leakage" currents due to incomplete cancellation were near 7.4 and 2.6%, respectively, of the total measured currents. Replacement of the 1 GΩ resistor with a 200 MΩ resistor provides an approximation of five ion channels, and the corresponding leakage currents at 120 and 30 Hz were about 1.4 and 0.6%, respectively.

It should be noted that there were numerous unsuccessful experimental runs during which, for example, the membrane would break, the hole in the partition would become "plugged" with fluid, overly large offset voltages developed, or there were so many channels that their number could not be reliably determined.

Figure 2 shows two examples of current–DC voltage characteristic curves for single channels recorded on different days. The curves are obtained using least square fitting software and are representative, in that small differences could be seen occasionally for positive membrane potentials. We note that there actually is a distribution of conductance values for the αHL channel [Menestrina, 1986] with the predominant value leading to a resistance of order 10^9 ohms for our conditions, as noted earlier. The nonlinearities in Figure 2 were typical, with the slope being greater for negative membrane potentials.

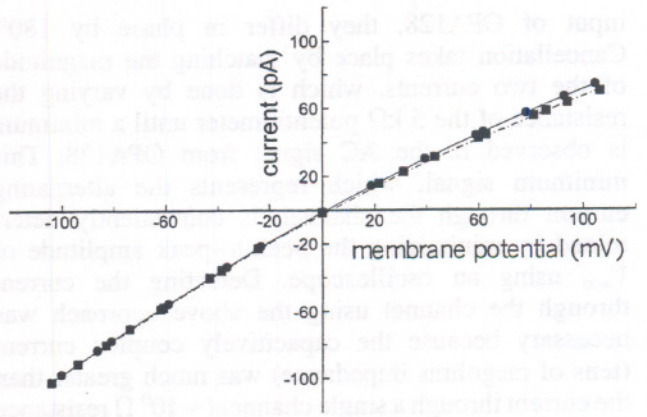

Fig. 2. Superposition of two current–DC voltage characteristic curves for single channels measured on different days. Occasionally, a difference in the current for positive membrane potentials was observed.

To examine whether multiple channels act as resistors in parallel, Figure 3 compares a current–DC voltage characteristic curve for five channels with that for a single channel (recorded on a different day) that has its current multiplied by a factor of 5. The excellent agreement of the five channel results with the behavior of actual resistors is perhaps fortuitous in light of the differences noted in Figure 2 and a relatively greater percentage of leakage current for the single channel case, but the data are persuasive for concluding that the current increases by the expected amount when multiple channels are created.

The current–DC voltage characteristic curve for five channels (Fig. 3) is shown again in Figure 4 with, for illustrative purposes, the superposition of a sinusoidal voltage at ±60 mV. If the channels are to behave as resistors (with the observed nonlinearities), the

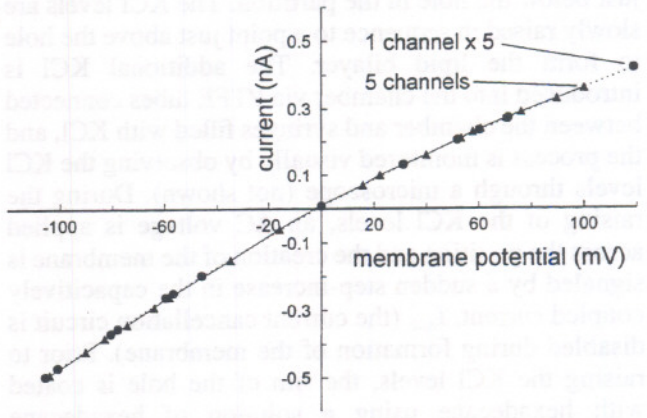

Fig. 3. Comparison of current–DC voltage characteristic curves for five channels and a single channel for which the current has been multiplied by a factor of 5.

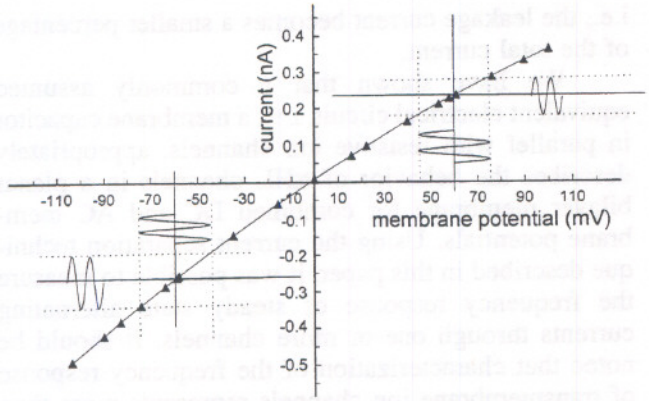

Fig. 4. Influence of nonlinearity of current–DC voltage characteristic curve on alternating current through channel for positive and negative membrane potentials.

different slopes for positive and negative membrane potentials should affect the peak-to-peak amplitude of the alternating current as shown in Figure 4. That is, the steeper slope for negative membrane potentials should lead to greater peak-to-peak currents compared to positive membrane potentials.

Table 1 shows comparisons between calculated peak-to-peak currents and measured values for different numbers of channels and membrane potentials. The calculated values are determined using equations of the form $a + b(\mathrm{mV}) + c(\mathrm{mV})^2$ obtained from the least squares fitting process, where a, b, and c are fitting constants, and mV is equal to the DC membrane potential $\pm$ the amplitude of the applied ac voltage, V_{in}. The calculated peak-to-peak current is just the difference between the two calculated current values. The measured peak-to-peak current value is determined using equation (2) for the rms value of I_{ac}, and assuming that V_{aco}, which is measured, is sinusoidal, i.e., I_{aco} is multiplied by $2^{3/2}$ to obtain the peak-to-peak current. Examination of the V_{aco} waveform using an oscilloscope confirmed that it was essentially sinusoidal.

Considering the experimental uncertainties noted earlier, most of the entries in Table 1 show good agreement between calculated and measured peak-to-peak current values. As indicated by the notes for the bottom four rows of Table 1, some calculations of the peak-to-peak current made use of single channel current–DC voltage characteristic curves obtained on days other than when I_{aco} was measured. The agreement with measured peak-to-peak current values was good for most cases. The less favorable agreement for case b may be explained by differences in the single channel current–DC voltage characteristic curves for positive membrane potentials (Fig. 2). The relatively poor agreement in the results for six channels with differences as large as 10% is difficult to explain and occurred during one experimental run.

Data for the frequency response of one, three, and five channels are presented in Figure 5. The rms current through ideal resistors should be independent of frequency and the data for the ion channels are in good agreement with such a response. Considering the single channel results in Figure 5, the data indicate (when numerical values are considered) an increase in current of about 12.5% as the frequency is varied between 30 and 120 Hz. Much of this change can be attributed to the imperfect cancellation of the capacitively coupled or "leakage" current. As noted earlier, an approximate simulation of the single channel case using a 1 GΩ resistor with a parallel capacitance of 55 pF indicated a current increase of 4.8% for the same change in frequency. When the capacitance was increased to 65.5 pF in the simulation, the leakage current increase was 8.3%.

As the number of channels increases in Figure 5, the percent change in the channel current decreases as

TABLE 1. Comparison of Calculated and Measured Peak-to-Peak Currents

Number of channels	Frequency (Hz)	Membrane potential (mV)	V_{in} (mV_{rms})	Calculated peak-to-peak current (pA)	Measured peak-to-peak current (pA)	Difference (%)
5	120/30	−58.0	10.0	138.0	141.9/139.2	2.8/0.9
5	120/80	58.0	10.0	98.5	102.3/100.1	3.9/1.6
6	120/50	−60.4	10.0	169.2	185.0/180.2	9.3/6.5
6	120/50	59.9	10.0	106.7	117.4/115.8	10.1/8.5
2	120	−60.3/60.5	10.0	56.1/40.3	58.5/41.3	4.3/2.5
5	30	59.2	10.0	97.6[a]	98.7	1.1
5	30	59.2	10.0	92.6[b]	98.7	6.6
3	30	−59.0	10.0	83.4[c]	85.7	2.8
5	30	59.2	10.0	97.9[d]	98.7	0.8

[a]Five channel current–DC voltage characteristic curve used for calculation.
[b]Single channel current–DC voltage characteristic curve multiplied by 5 used for calculation.
[c]Single channel current–DC voltage characteristic curve (note b) multiplied by 3 used for calculation.
[d]Single channel current–DC voltage characteristic curve recorded on different day (from note b) multiplied by 5 used for calculation.

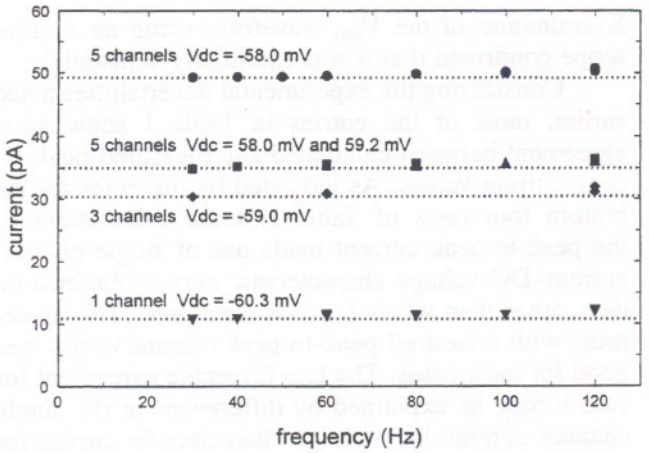

Fig. 5. Frequency response of current through single and multiple channels. The combined current data for 5 channels with slightly different positive membrane potentials (58 and 59.2 mV) were obtained on different days.

the frequency is increased. For the three channel and five channel (Vdc = 58 mV and 59.2 mV) cases, the current increase was near 4% as the frequency was increased from 30 to 120 Hz. The corresponding current data for five channels ($V_{DC} = -58.0$ mV) indicates a change of about 2.4%. Simulation of the membrane and ion channels with resistors and capacitors resulted in similar changes as the frequency was varied.

Using a lock-in amplifier, the degree of linearity in the relation between the applied rms AC voltage V_{in} and V_{aco} was checked on one occasion for seven channels at a frequency of 100 Hz. The linear regression correlation coefficient between the two voltages was 0.999999 for applied voltages between 0.88 and 10.0 mV.

SUMMARY AND CONCLUSIONS

The results presented in Figures 2–5 and Table 1 indicate that, for the most part, the channels under AC and DC voltage conditions act as resistors in parallel with a capacitor, if one ignores the lack of linearity in the current–DC voltage characteristic curves and possible variations in the conductance of the channels. The frequency response of the channels from 30 to 120 Hz corresponds well to that of resistors if the uncertainty associated with incomplete cancellation of the capacitively coupled current is taken into account. The decrease in the *change* of rms current as the frequency is increased for multiple channels, versus a single channel, is expected. The reason is that the capacitively coupled leakage current remains constant, while the current through multiple resistors is greater, i.e., the leakage current becomes a smaller percentage of the total current.

We have shown that a commonly assumed equivalent electrical circuit, i.e., a membrane capacitor in parallel with resistive ion channels, appropriately describes the behavior of αHL channels in a planar bilayer membrane for combined DC and AC membrane potentials. Using the current separation technique described in this paper, it was possible to measure the frequency response of steady state alternating currents through one or more channels. It should be noted that characterization of the frequency response of transmembrane ion channels represents more than "properties of materials" type metrology. As already indicated, in contrast to capacitively coupled currents through membranes, alternating currents through channels represent transport of ions through membranes, and their frequency response may be of interest for researchers conducting bioeffects studies. For example, it is well known that pulsed magnetic fields are sometimes used for healing broken bones [Jain and Gupta, 1994; McLeod et al., 1995]. While the mechanism for their therapeutic effects are not well understood, pulsed magnetic fields are known to induce voltages that can appear as membrane potentials at the surface of cells. Because these induced potentials can be rich in frequency content, knowledge of the frequency response of ion channels at the cell surface might be helpful in understanding perhaps which frequency components are "biologically active."

The membrane/channel system that was studied in this paper appears ideal for use in the further development of the current separation technique. For example, it would be of interest, with improved electronics, to examine the frequency response at higher frequencies, consider waveforms other than sinusoidal, and to perform linearity checks for much smaller alternating potentials than considered here. The influence of different pH and molarity values, which can influence the current–voltage characteristic curves [Kasianowicz and Bezrukov, 1995], would also be of interest. Experience gained via studies of the αHL channel could be of value for studies of other voltage-gated channels as indicated above.

ACKNOWLEDGMENT

This study was funded in part by the Office of Utility Technologies, U.S. Department of Energy.

REFERENCES

Benavente J, Oleinikova M, Muñoz M, Valiente M. 1998. Characterization of novel activated composite membranes by impedance spectroscopy. J Electroanal Chem 451:173–180.

Bezrukov SM, Kasianowicz JJ. 1993. Current noise reveals protonation kinetics and number of ionizable sites in an open protein ion channel. Phys Rev Lett 70:2352–2355.

Bezrukov SM, Kasianowicz JJ. 1997. Charge state of an ion channel controls neutral polymer entry into its pore. Eur Biophys J 6:471–476.

Bezrukov SM, Vodyanoy I, Brutyan RA, Kasianowicz JJ. 1996. Dynamics and free energy of polymers partitioning into a nanoscale pore. Macromolecules 29:8517–8522.

Cescatti L, Pederzollli C, Menestrina, G. 1991. Modification of lysine residues of *staphylococcus aureus* α-toxin: effects on channel-forming properties. J Membr Biol 119:53–64.

Covington AK, Zhou D-M. 1992. Ac impedance properties of eth1001-based calcium ion selective membranes. Electrochim Acta 37:2691–2694.

Deslouis C, Musiani MM, Tribollet B. 1994. AC impedance study of transport processes in polyaniline membranes. J Phys Chem 98:2936–2940.

Durney CH, Kaminski M, Anderson A, Bruckner-Lea C, Janata J, Rappoport C. 1992. Investigation of AC-DC magnetic field effects in planar phospholipid bilayers. Bioelectromagnetics 13:19–33.

Galt S, Sandblom J, Hamnerius Y, Höjevik P, Saalman E, Nordén B. 1993. Experimental search for combined AC and DC magnetic effects on ion channels. Bioelectromagnetics 14:315–327.

Henrickson, SE, Misakian M, Robertson B, Kasianowicz JJ. 2000. Asymmetric driven DNA transport in a nanometer-scale pore. Phys Rev Lett 85:3057–3060.

Hille B. 1991. Ionic channels of excitable membranes. Sunderland, MA: Sinauer Associates, Inc., Chapter 1.

Jain VK, Gupta T. 1994. Recent trends in bone-growth by electrical-stimulation. IETE Tech Rev 11:55–62.

Kasianowicz JJ, Burden DL, Han L, Cheley S, Bayley H. 1999. Genetically engineered metal ion binding sites on the outside of a channel's transmembrane β-barrel. Biophys J 76:837–845.

Kasianowicz JJ, Bezrukov SM. 1995. Protonation dynamics of the α-toxin channel from spectral analysis of pH dependent current fluctuation. Biophys J 69:94–105.

Kasianowicz JJ, Brandin E, Branton D, Deamer DW. 1996. Characterization of individual polynucleotide molecules using a membrane channel. Proc Natl Acad Sci USA 93:13770–13773.

Kasianowicz JJ, Burden DL, Han LC, Cheley S, Bayley H. 1999. Genetically engineered metal ion binding sites on the outside of a channel's transmembrane β-barrel. Biophys J 76:837–845.

Krasilnikov OV, Sabirov RZ, Ternovsky VI, Merzliak PG, Tashmukhamedov BA. 1988. The structure of *Staphylococcus aureus* α-toxin-induced ionic channels. Gen Physiol Biophys 7:467–473.

Macdonald JR, editor. 1987. Impedance spectroscopy. New York, NY: John Wiley & Sons.

Menestrina G. 1986. Ionic channels formed by *Staphylococcus aureus* alpha-toxin: Voltage-dependent inhibition by divalent and trivalent cations. J Membr Biol 90:177–190.

McLeod KJ, Rubin CT, Donahue HJ. 1995. Electromagnetic fields in bone repair and adaptation. Radio Sci 30:233–244.

Montal M, Mueller P. 1972. Formation of bimolecular membranes from lipid monolayers and a study of their electrical properties. Proc Nat Acad Sci USA 69:3561–3566.

Peyton AJ, Walsh V. 1993. Analog electronics with Op Amps. New York, NY; Cambridge University Press, p 38.

Song LZ, Hobaugh MR, Shustak C, Cheley S, Bayley H, Gouaux JE. 1996. Structure of staphylococcal alpha-hemolysin, a heptameric transmembrane pore. Science 274:1859–1866.